Plasmon modes of spatially separated double-layer graphene

E. H. Hwang and S. Das Sarma
Condensed Matter Theory Center, Department of Physics, University of Maryland, College Park, Maryland 20742-4111, USA
(Received 10 September 2009; published 6 November 2009)

We derive the plasmon dispersion in doped double-layer graphene (DLG), made of two parallel graphene monolayers with carrier densities n_1 and n_2, respectively, and an interlayer separation of d. The linear chiral gapless single-particle energy dispersion of graphene leads to DLG plasmon properties with several unexpected experimentally observable characteristic features such as a nontrivial influence of an undoped ($n_2=0$) layer on the DLG plasmon dispersion and a strange influence of the second layer even in the weak-coupling $d\to\infty$ limit. At long wavelengths ($q\to 0$), the density dependence of the plasma frequencies is different from the usual two-dimensional (2D) electron system with quadratic energy dispersion. Our predicted DLG plasmon properties clearly distinguish graphene from the extensively studied usual parabolic 2D electron systems.

DOI: 10.1103/PhysRevB.80.205405 PACS number(s): 73.20.Mf, 71.45.Gm, 81.05.Uw

I. INTRODUCTION

Graphene, a two-dimensional (2D) layer of carbon atoms arranged in a honeycomb lattice, has attracted a great deal of attention because of its unique electronic properties arising from its chiral, gapless, and linear band dispersion.[1] Of particular importance and fundamental interest are those graphene properties, which are *qualitatively* different from the behavior of electrons (or holes) in the extensively studied 2D semiconductor systems. Some of these unique graphene properties[1] are its "half-integral" integer-quantized Hall effect, a carrier mobility independent of carrier density away from the charge neutrality point (i.e., the Dirac point), and the finite minimum conductivity around the Dirac point without any obvious metal-insulator transition.

It is known[2] that the long-wavelength plasmon frequency of graphene is explicitly nonclassical with the plasma frequency being proportional to $1/\sqrt{\hbar}$, i.e., the long-wavelength plasmon frequency of graphene is necessarily quantum with "$\hbar$" appearing manifestly in the long-wavelength plasma frequency. By contrast the long-wavelength plasma frequency of ordinary electron liquids is classical, and quantum effects show up only as nonlocal corrections in higher order wave vector dispersion of the plasmon mode.[3] In this paper, we predict a new collective property of graphene electrons, which distinguishes graphene qualitatively from the semiconductor-based parabolic 2D electron systems. We find the surprising result that the plasma modes of an interacting double-layer graphene (DLG) system are completely different from the double-layer semiconductor quantum well plasmons.[4] Our finding is unexpected and interesting because the collective plasmon excitations arise from the long-range Coulomb interaction, which is the same in graphene and parabolic 2D systems. The DLG plasmon properties are experimentally observable and should have important consequences for the many-body effects in doped multilayer graphene structures.

Plasma modes of 2D double-layer structures have been extensively studied ever since the existence of an undamped acoustic plasmon mode was predicted[4] in semiconductor double quantum well systems. It is known that when the two 2D layers are put in close proximity with a high-insulating barrier between them to prevent interlayer tunneling, the 2D plasmons are coupled by the interlayer Coulomb interaction leading to the formation[4] of two branches of longitudinal collective excitation spectra called the optical plasmon (OP) $\omega_+\sim q^{1/2}$, where q is the 2D wave vector and the acoustic plasmon (AP) $\omega_-\sim q$, where the density fluctuations in each component oscillate in-phase OP and out-of-phase AP modes, respectively, relative to each other, assuming the two charge components to be the same. These collective modes of the double-layer structures, which have been directly experimentally observed,[5] play important roles in the many-body properties such as screening and drag.[6,7]

Here we consider the experimentally relevant issue of the collective-mode dispersion in DLG formed by two parallel single-layer graphene (SLG) separated by a distance d. The DLG is fundamentally different from the well-studied bilayer graphene[8] because there is no interlayer tunneling, and there is only interlayer Coulomb interaction. Spatially separated two-component DLG can be fabricated by folding an SLG over a high-insulating substrate.[9]

We calculate the DLG plasmon modes and their loss functions (spectral strength). We find many intriguing and unexpected features of coupled plasmon modes and their Landau damping in DLG. We recover in the long-wavelength ($q\to 0$) limit the well-known optical ($\omega_+\approx\omega_0^+q^{1/2}$) and acoustic ($\omega_-\approx\omega_0^-q$) plasmons, but the density dependence of the plasma frequency are given by $(\omega_0^+)^2\propto\sqrt{n_1}+\sqrt{n_2}$ and $(\omega_0^-)^2\propto\sqrt{n_1n_2}/(\sqrt{n_1}+\sqrt{n_2})$ compared to $(\omega_0^+)^2\propto N$ and $(\omega_0^-)^2\propto n_1n_2/N$ in the ordinary 2D system, where $N=n_1+n_2$. When the interlayer Coulomb coupling is weak (i.e., for large separations, $k_Fd\gg 1$) the undamped DLG modes ($\omega_\pm$) become degenerate and have the same frequency as the uncoupled SLG plasmon,[10] but inside the interband Landau damping regime this degenerate mode splits into two coupled modes. In the strong-coupling regime ($k_Fd\ll 1$), the ω_- mode approaches the intraband electron-hole continuum (i.e., $\omega_-\to v_Fq$) and is overdamped, but the ω_+ mode is shifted to higher frequency and in the long-wavelength limit becomes the SLG plasmon with a density $N=n_1+n_2+2\sqrt{n_1n_2}$ instead of the density $N=n_1+n_2$ as happens in regular 2D double-layer systems. We also find that the DLG plasmon modes are heavily damped even in the long-wavelength

limit when the two layers have unequal density, even when one layer is undoped (i.e., $n_2=0$). We believe that our predictions may be easily observable via inelastic light-scattering spectroscopy,[11] frequency-domain far-infrared (or microwave) spectroscopy,[12] or inelastic electron-scattering spectroscopy.[13,14] The plasmons we discuss in this paper are produced by electrons (holes) in the conduction (valence) band. These low-energy plasmons are different from the very high-energy valence-band plasmons involving all electrons (where the non-Dirac band structure would matter).[14]

The paper is organized as follows. In Sec. II the generalized random-phase approximation (RPA) is presented to calculate the plasmon modes of spatially separated double-layer graphene. Section III presents the results of the calculations. We conclude in Sec. IV with a discussion.

II. THEORY

The plasmon modes are given by the poles of the density-density correlation function, or equivalently by the zeros of the dynamical dielectric function. For a double-layer system the collective modes are given by the zeros of the generalized dielectric tensor ϵ_{lm}, where $l,m=1$ or 2 with 1,2 denoting the two layers.[4] The dielectric function is obtained within the mean-field random-phase approximation in our theory, i.e.,

$$\epsilon_{lm}(q,\omega) = \delta_{lm} - v_{lm}\Pi_m, \tag{1}$$

and the two-component determinantal equation becomes

$$\epsilon(q,\omega) = [1 - v_{11}(q)\Pi_1(q,\omega)][1 - v_{22}(q)\Pi_2(q,\omega)] - v_{12}(q)v_{21}(q)\Pi_1(q,\omega)\Pi_2(q,\omega), \tag{2}$$

where $v_{ll}(q)$ and $v_{lm}(q)$ are, respectively, the intralayer and interlayer Coulomb interaction matrix elements. In our model, $v_{ll}(q)=2\pi e^2/(\kappa q)$; $v_{lm}(q)=v_{ll}(q)\exp(-qd)$, with κ as the background lattice dielectric constant. Finally, $\Pi_l(q,\omega)$ in Eq. (2) is the noninteracting SLG polarizability function given by[10]

$$\Pi_l(q,\omega) = -\frac{g}{L^2}\sum_{\mathbf{k}ss'}\frac{f_{s\mathbf{k}} - f_{s'\mathbf{k}'}}{\omega + \epsilon_{s\mathbf{k}} - \epsilon_{s'\mathbf{k}'} + i\eta}F_{ss'}(\mathbf{k},\mathbf{k}'), \tag{3}$$

where $g=g_s g_v$ (with $g_s=2$ and $g_v=2$ being spin and valley degeneracies) $\mathbf{k}'=\mathbf{k}+\mathbf{q}$, $s,s'=\pm 1$ denote the band indices, $\epsilon_{s\mathbf{k}}=sv_F|\mathbf{k}|$ (v_F being the Fermi velocity of graphene and $\hbar=1$ throughout this paper), and $F_{ss'}(\mathbf{k},\mathbf{k}')$ is the overlap of states and given by $F_{ss'}(\mathbf{k},\mathbf{k}')=\frac{1}{2}(1+ss'\cos\theta)$, where θ is the angle between $\mathbf{k}$ and $\mathbf{k}'$, and f_{sk} is the Fermi distribution function, $f_{s\mathbf{k}}=\{\exp[\beta(\epsilon_{s\mathbf{k}}-\mu_l)]+1\}^{-1}$, with $\beta=1/k_BT$ and μ_l being the chemical potential of lth layer. In the long-wavelength limit ($q\to 0$) the polarizability becomes[10]

$$\Pi_l(q,\omega) = \frac{gk_{F_l}}{4\pi v_F}\frac{q^2}{\omega^2}\left(1 - \frac{\omega}{4E_{F_l}}\ln\frac{2E_{F_l}+\omega}{2E_{F_l}-\omega}\right), \tag{4}$$

where $k_{F_l}(E_{F_l}=v_Fk_{F_l})$ is the Fermi wave vector (Fermi energy) of the lth layer.

The analytical formula for the long-wavelength plasmon dispersion can be obtained in the general situation, where the two layers have different Fermi wave vectors and Fermi energies by virtue of having different densities n_1,n_2. From Eqs. (2) and (4) it is possible to obtain the following long-wavelength plasma modes of the coupled DLG

$$\omega_+^2(q\to 0) = 2r_s v_F^2(k_{F_1}+k_{F_2})q, \tag{5a}$$

$$\omega_-^2(q\to 0) = \frac{4r_s v_F^2 k_{F_1}k_{F_2}d}{k_{F_1}+k_{F_2}}q^2, \tag{5b}$$

where $r_s=e^2/\kappa v_F$ is the effective graphene fine-structure constant. Thus, one recovers in a straightforward fashion the well-known optical ($\omega_+\sim q^{1/2}$) and acoustic ($\omega_-\sim q$) plasmons of a double-layer system. In addition, we have the density dependence of DLG plasmons as

$$\omega_+(q\to 0) \propto (\sqrt{n_1}+\sqrt{n_2})^{1/2}\sqrt{q}, \tag{6a}$$

$$\omega_-(q\to 0) \propto \left(\frac{\sqrt{n_1 n_2}}{\sqrt{n_1}+\sqrt{n_2}}\right)^{1/2} q, \tag{6b}$$

which are different from the density dependence of the corresponding plasmon dispersion in ordinary 2D systems,[4] where the ω_+^2 depends on the total 2D electron density $N=n_1+n_2$ (i.e., $\omega_+^2/q\propto N$) and $\omega_-^2/q\propto n_1n_2/N$. Note that when interlayer hopping is included in a bilayer system, the in-phase plasmon mode is qualitatively unaffected by tunneling. However, the out-of-phase plasmon mode develops a long-wavelength gap (depolarization shift) (Ref. 15) in the presence of tunneling, i.e., $\omega_-(q\to 0)=(2t)^2(1+4r_sk_Fd)$, where t is the interlayer hopping.

III. RESULTS

In Fig. 1 we show the calculated DLG plasmon dispersions ($\omega_\pm$) for equal densities of $n_1=n_2=10^{12}$ cm^{-2} and several layer separations. The plasmon mode dispersion of the uncoupled SLG with the same density is shown as the dot-dashed line. In Fig. 1, we also show the electron-hole continua or single-particle excitation (SPE) region, which determines the decay (Landau damping) of the plasmon at a given frequency and wave vector. If the collective mode lies inside the SPE continua, we expect the mode to be Landau-damped. The SPE continuum is defined by the nonzero value of the imaginary part of the total dielectric function, $\mathrm{Im}[\epsilon(q,\omega)]\neq 0$, because the damping of the plasmon by emitting an electron-hole single-pair excitation is allowed in the region of nonzero $\mathrm{Im}[\Pi(q,\omega)]$. For graphene, both intraband and interband SPE transitions are possible,[10] and the boundaries (dashed lines) are given in Fig. 1. Due to the phase-space restriction, the interband SPE continuum opens a gap in the long-wavelength region satisfying the following condition: $v_Fq<\omega<2E_F-v_Fq$, in which the undamped plasmon modes exist. Since the normalized plasmon mode dispersion in E_F scales with normalized Fermi wave vector, our calculated results of Fig. 1 apply also for all other densities.

As shown in Fig. 1(a), for a small spatial separation ($k_Fd<1$), the frequency of the acoustic mode ω_- decreases compared with the uncoupled mode and approaches the up-

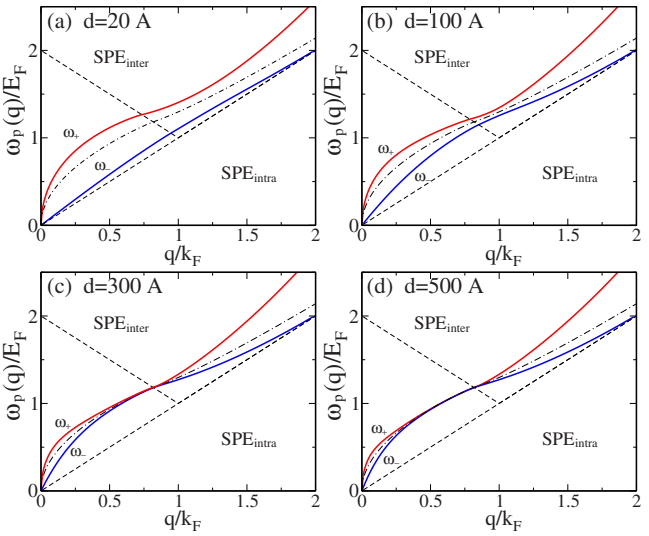

FIG. 1. (Color online) Calculated plasmon mode dispersions of coupled DLG for a fixed density and several layer separations. The upper (lower) solid line indicates the in-phase mode ω_+ (the out-of-phase mode ω_-). Here we use the parameters: $n_1=n_2=10^{12}$ cm^{-2} and (a) $d=20$ Å($k_Fd=0.35$), (b) $d=100$ Å($k_Fd=1.8$), (c) $d=300$ Å($k_Fd=5.3$), and (d) $d=500$ Å($k_Fd=8.9$). The dot-dashed line indicates the plasmon mode dispersion of SLG with the same density. The dashed lines indicate the boundaries of SPEs (Landau damping region for intraband and interband electron-hole excitations).

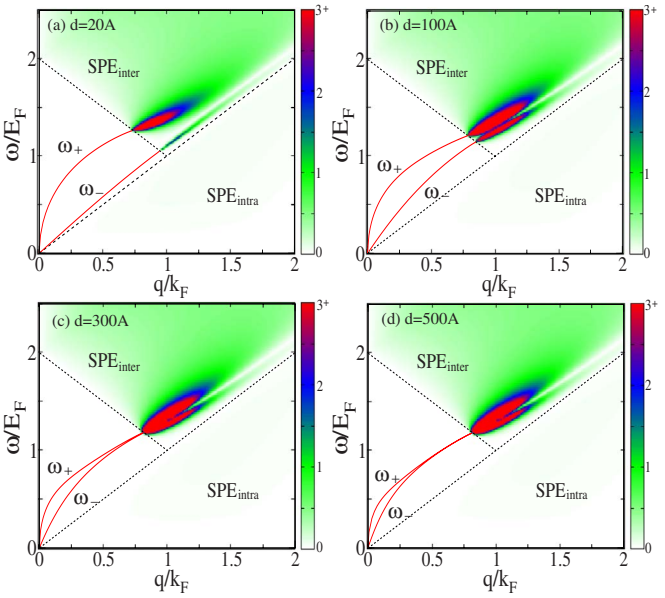

FIG. 2. (Color online) The density plots of DLG loss function $\{-\mathrm{Im}[\epsilon(q,\omega)^{-1}]\}$ in (q,ω) space for fixed densities of $n_1=n_2=10^{12}$ cm^{-2} and several layer separations $d=20,100,300,500$ Å. The dashed lines indicate the boundaries of SPEs and the solid lines represent the undamped plasmon modes (δ-function peaks in the loss function).

per boundary of intraband SPE (i.e., $\omega=v_Fq$), while the optical mode ω_+ shifts to higher energy. Especially, as $d\to 0$, the ω_- mode becomes degenerate with the electron-hole continuum and loses its identity (i.e., $\omega_-\to v_Fq$). On the other hand, the ω_+ mode becomes the SLG plasmon mode with a density $N=n_1+n_2+2\sqrt{n_1n_2}$ in the long-wavelength limit. This is very interesting because, when the two layers with densities n_1,n_2 become one combined system ($d\to 0$), the optical plasmon mode (ω_+) should correspond to the SLG plasmon of total density $N=n_1+n_2$, which is precisely what happens in regular 2D double-layer system. As the spatial separation increases the optical (acoustic) plasmon frequency decreases (increases) slowly and the mode coupling occurs at the boundary of interband SPE [see Fig. 1(b)]. As d increases further the two modes become degenerate below the SPE$_{\mathrm{inter}}$ (i.e., in the undamped region), but the degenerate mode is divided into two coupled modes inside interband SPE [see Figs. 1(c) and 1(d)]. For infinite separation, the two modes become uncoupled and have the dispersion of SLG plasmon with the density $n=n_1=n_2$.

In Fig. 2 we show the calculated DLG loss function {i.e., $-\mathrm{Im}[\epsilon(q,\omega)^{-1}]$} plotted in q-ω space. The loss function is related to the dynamical structure factor $S(q,\omega)$ by $S(q,\omega)\propto -\mathrm{Im}[\epsilon(q,\omega)^{-1}]$. The dynamical structure factor gives a direct measure of the spectral strength of the various elementary excitations. Thus, our calculated loss function can be measured in experiments such as inelastic electron and Raman-scattering spectroscopies. When both $\mathrm{Re}[\epsilon]$ and $\mathrm{Im}[\epsilon]$ become zero (i.e., $\epsilon(q,\omega)=0$, which defines the plasmon mode), the imaginary part of the inverse dielectric function, $\mathrm{Im}[\epsilon(q,\omega)^{-1}]$, is a δ function with the strength $W(q)=\pi\{|\partial\,\mathrm{Re}[\epsilon(q,\omega)]/\partial\omega|_{\omega=\omega_p(q)}\}^{-1}$, where $\omega_p(q)$ is the plasmon dispersion. Thus the undamped plasmon shows up as a well-defined δ-function peak in the loss function. The damped plasmon, however, corresponds to a broadened peak in the loss function—for larger broadening, the plasmon is overdamped and there is no peak in the loss function.

In Fig. 2 we show the $-\mathrm{Im}[\epsilon(q,\omega)^{-1}]$ in density plots, where darkness represents the mode spectral strength. The solid lines indicate the δ-function peaks and correspond to the well-defined undamped plasmon modes. The intraband electron-hole SPE continuum shows up as weak broad (incoherent) structure in Fig. 2 and carries small spectral weight. For a small spatial separation only the in-phase mode ω_+ carries any significant spectral strength. As d increases the out-of-phase mode carries substantial spectral weight even at long wavelengths ($q\to 0$). Both $\omega_\pm$ modes in general carry finite spectral weights and should be observable in experiments.[11–14] Since both $\omega_\pm(q)$ are greater than $\omega=v_Fq$ for all q, which is the upper boundary of the intraband electron-hole pair continuum, we expect these modes not to decay by intraband electron-hole pairs. But the modes enter into interband SPE at finite q_c, which is given by the condition, $\omega_\pm(q_c)=2E_F-v_Fq_c$. If $q>q_c$, $\epsilon(q,\omega_\pm)$ has a finite imaginary part and the plasmon modes become damped consequently (Landau damping). The plasmon mode inside the Landau damping region decays by emitting interband electron-hole pairs, which is now allowed by energy-momentum conservation. Near the boundary of the interband SPE the mode damping is not significant.

In Fig. 3 we show the calculated DLG plasmon mode dispersion and the corresponding loss function $\{-\mathrm{Im}[\epsilon(q,\omega)^{-1}]\}$ for unequal layer densities at fixed layer

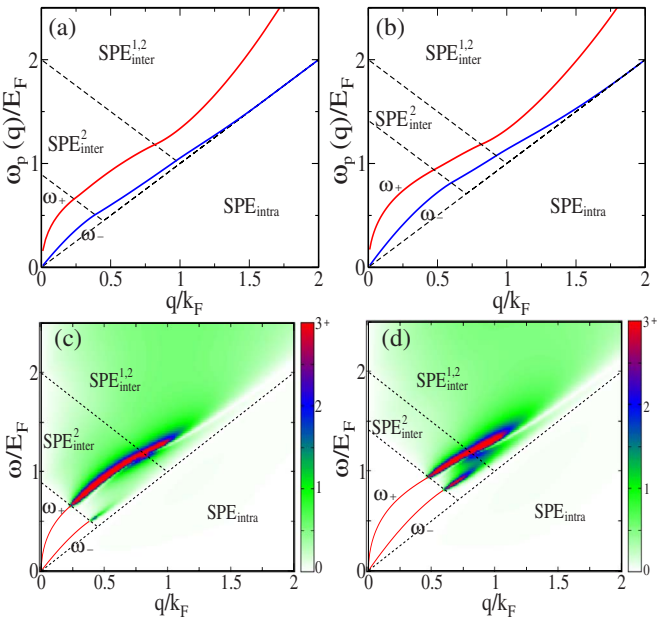

FIG. 3. (Color online) Calculated plasmon mode dispersions and $-\mathrm{Im}[\epsilon(q,\omega)^{-1}]$ of DLG for fixed layer separation ($d=100$ Å) and for different layer densities. Here we use $n_1=10^{12}$ cm^{-2} and in (a) and (c) $n_2/n_1=0.2$ and in (b) and (d) $n_2/n_1=0.5$.

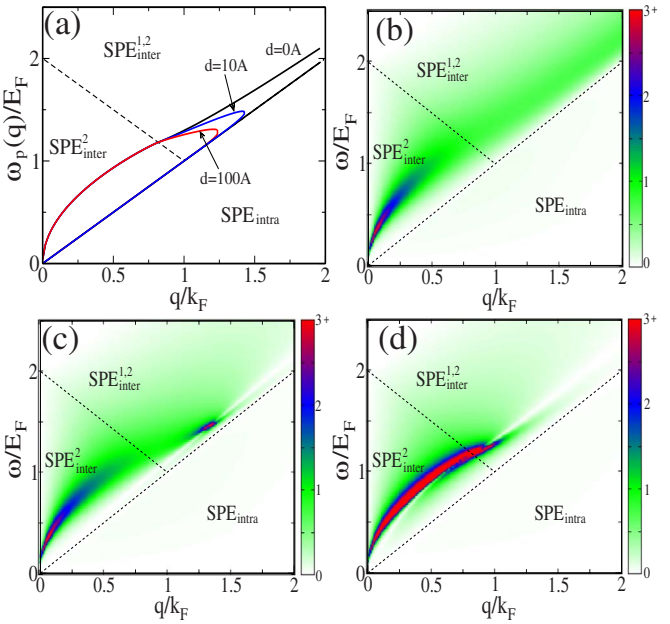

FIG. 4. (Color online) (a) Calculated plasmon mode dispersions of DLG for different layer separations for $n_2/n_1=0$ (i.e., $n_2=0$ and $n_1=10^{12}$ cm^{-2}), and corresponding loss functions $\{-\mathrm{Im}[\epsilon(q,\omega)^{-1}]\}$ for (b) $d=0$ Å, (c) $d=10$ Å, and (d) $d=100$ Å.

separation ($d=100$ Å). As the layer densities are different the undamped plasmon region becomes smaller in q-ω space. As q increases the modes first enter SPE$^2_{\mathrm{inter}}$ at smaller q_c and decay by producing interband electron-hole pairs in layer two. As q increases further the modes enter into SPE$^1_{\mathrm{inter}}$ and decay by exciting interband electron-hole pairs in both layers. As the density imbalance increases (i.e., n_2/n_1 decreases) the acoustic mode (ω_-) approaches the boundary of interband SPE and loses its spectral strength severely. But the in-phase mode ω_+ remains as a well-defined peak inside SPE$^2_{\mathrm{inter}}$.

In Fig. 4(a) we show the DLG plasmon modes in the case of $n_2/n_1=0$, i.e., layer two is undoped ($n_2=0$) and layer one has a finite density $n_1=10^{12}$ cm^{-2}. Even though there are no free carriers in layer two we have two coupled plasmon modes {i.e., we find two zeros in $\mathrm{Re}[\epsilon(q,\omega)]$}: one ($\omega_+$) is above SPE$_{\mathrm{intra}}$ and the other (ω_-) is degenerate with the boundary of SPE$_{\mathrm{intra}}$ [i.e., $\omega(q)=v_F q$]. More interestingly, when the layer separation is finite (i.e., $d\neq 0$) the two plasmons merge at a finite wave vector $q_m(>k_F)$. We find that the mode dispersion and q_m are unchanged when $d>100$ Å. As $d\to 0$ the dispersion of ω_+ becomes exactly that of SLG plasmon with the same density, and the two modes $\omega_\pm$ never meet. In Figs. 4(b)–4(d) we show the loss function of DLG corresponding to Fig. 4(a). Since all modes are inside of SPE$^2_{\mathrm{inter}}$, there is no undamped Landau region, so the modes are damped by producing interband electron-hole pairs in layer two even in the long-wavelength limit. The loss function shows that ω_- does not carry any spectral weight, and all spectral weight is carried by ω_+. For $d=0$, the ω_+ mode becomes a well-defined peak only in the long-wavelength limit and appears as a very broad peak for high wave vectors. As the separation increases, ω_+ is well defined below q_m even inside SPE$_{\mathrm{inter}}$ and manifests well-defined spectral peaks. Note that there is no significant spectral weight for $q>q_m$.

IV. CONCLUSION

In conclusion, we investigate theoretically the dynamical response of double-layer graphene, made of two parallel graphene monolayers with carrier densities n_1 and n_2, respectively, and an interlayer separation of d. We derive the plasmon dispersion and the loss function of DLG. The linear chiral gapless single-particle energy dispersion of graphene leads to DLG plasmon properties with several unexpected experimentally observable characteristic features such as a nontrivial influence of an undoped ($n_2=0$) layer on the DLG plasmon dispersion and a strange influence of the second layer even in the weak-coupling $d\to\infty$ limit. At long wavelengths ($q\to 0$), the density dependence of the plasma frequencies is different from the usual 2D electron system with quadratic energy dispersion. Our predicted DLG plasmon properties clearly distinguish graphene from the extensively studied usual parabolic 2D electron systems. We believe that our predictions may be easily observable via inelastic light-scattering spectroscopy, frequency-domain far-infrared (or microwave) spectroscopy, or inelastic electron-scattering spectroscopy.

ACKNOWLEDGMENTS

This work is supported by DOE-Sandia and US-ONR. We acknowledge the hospitality of the KITP at UCSB where this research was initiated.

[1] A. H. Castro Neto, F. Guinea, N. M. R. Peres, K. S. Novoselov, and A. K. Geim, Rev. Mod. Phys. **81**, 109 (2009).
[2] S. Das Sarma and E. H. Hwang, Phys. Rev. Lett. **102**, 206412 (2009).
[3] D. Pines and P. Nozieres, *The Theory of Quantum Liquids* (Benjamin, New York, 1966); G. D. Mahan, *Many Particle Physics* (Plenum, New York, 2000).
[4] S. Das Sarma and A. Madhukar, Phys. Rev. B **23**, 805 (1981); S. Das Sarma and J. J. Quinn, *ibid.* **25**, 7603 (1982); J. K. Jain and S. Das Sarma, *ibid.* **36**, 5949 (1987).
[5] N. P. R. Hill, J. T. Nicholls, E. H. Linfield, M. Pepper, D. A. Ritchie, G. A. C. Jones, Ben Yu-Kuang Hu, and K. Flensberg, Phys. Rev. Lett. **78**, 2204 (1997); D. S. Kainth, D. Richards, A. S. Bhatti, H. P. Hughes, M. Y. Simmons, E. H. Linfield, and D. A. Ritchie, Phys. Rev. B **59**, 2095 (1999).
[6] A. P. Jauho and H. Smith, Phys. Rev. B **47**, 4420 (1993); K. Flensberg and Ben Yu-Kuang Hu, *ibid.* **52**, 14796 (1995).
[7] J. A. Seamons, C. P. Morath, J. L. Reno, and M. P. Lilly, Phys. Rev. Lett. **102**, 026804 (2009); A. F. Croxall, K. Das Gupta, C. A. Nicoll, M. Thangaraj, H. E. Beere, I. Farrer, D. A. Ritchie, and M. Pepper, *ibid.* **101**, 246801 (2008).
[8] E. McCann and V. I. Fal'ko, Phys. Rev. Lett. **96**, 086805 (2006); M. Koshino and T. Ando, Phys. Rev. B **73**, 245403 (2006); E. H. Hwang and S. Das Sarma, Phys. Rev. Lett. **101**, 156802 (2008).
[9] H. Schmidt, T. Ludtke, P. Barthold, E. McCann, V. I. Fal'ko, and R. J. Haug, Appl. Phys. Lett. **93**, 172108 (2008).
[10] E. H. Hwang and S. Das Sarma, Phys. Rev. B **75**, 205418 (2007); B. Wunsch, T. Stauber, F. Sols, and F. Guinea, New J. Phys. **8**, 318 (2006).
[11] A. Pinczuk, M. G. Lamont, and A. C. Gossard, Phys. Rev. Lett. **56**, 2092 (1986); G. Fasol, N. Mestres, H. P. Hughes, A. Fischer, and K. Ploog, *ibid.* **56**, 2517 (1986); D. Olego, A. Pinczuk, A. C. Gossard, and W. Wiegmann, Phys. Rev. B **25**, 7867 (1982).
[12] S. J. Allen, D. C. Tsui, and R. A. Logan, Phys. Rev. Lett. **38**, 980 (1977).
[13] Yu Liu, R. F. Willis, K. V. Emtsev, and Th. Seyller, Phys. Rev. B **78**, 201403(R) (2008).
[14] T. Eberlein, U. Bangert, R. R. Nair, R. Jones, M. Gass, A. L. Bleloch, K. S. Novoselov, A. Geim, and P. R. Briddon, Phys. Rev. B **77**, 233406 (2008); J. Lu, K. P. Loh, H. Huang, W. Chen, and A. T. S. Wee, *ibid.* **80**, 113410 (2009); C. Kramberger, R. Hambach, C. Giorgetti, M. H. Rummeli, M. Knupfer, J. Fink, B. Buchner, L. Reining, E. Einarsson, S. Maruyama, F. Sottile, K. Hannewald, V. Olevano, A. G. Marinopoulos, and T. Pichler, Phys. Rev. Lett. **100**, 196803 (2008); A. Nagashima, K. Nuka, H. Itoh, T. Ichinokawa, C. Oshima, S. Otani, and Y. Ishizawa, Solid State Commun. **83**, 581 (1992).
[15] S. Das Sarma and E. H. Hwang, Phys. Rev. Lett. **81**, 4216 (1998).